Coloured Particle-in-Cell simulations of non-Abelian plasma dynamics in glasma

Graduate School of Science, Hiroshima University
Department of Physical Science

M162632 Tomohiro Honda

Supervisor : Prof. Toru Sugitate
Chief examiner : Prof. Toru Sugitate
Second examiner : Associate Prof. Takuya Morozumi

April 2, 2018

Abstract

Ultrarelativistic heavy ion collisions create quark gluon plasma(QGP), a deconfined state of quarks and gluons. There have been a lot of experiments to understand the nature of QGP. From these attempts, elliptic flow of QGP was found and it is an evidence for a collective motion of partons. The results are consistent with hydrodynamical simulations, therefore, it is considered that QGP is in a local equilibrium state. Its thermalisation process, however, is still one of the big questions in heavy ion collisions. One possible explanation is that plasma instabilities take significant role in thermalising preliminary matter, glasma. Hence, it is important to understand the plasma dynamics in glasma for exploring the very beginning of heavy ion collisions. In this thesis, I investigate fundamental physics of plasma dynamics in glasma. Assuming high energy limit, high momentum gluons can be treated as plasma particles, low momentum ones as background fields. For basics equations of calculation, I adopted one dimensional Wong-Yang-Mills equations, based on Vlasov equation and Yang-Mills equations. Analysing kinetic evolution of plasma numerically, I implemented coloured Particle-in-Cell(PIC) method which is the expansion of PIC method commonly used for plasma simulations.

I set initial condition such as counter flow of particles and a few types of electro-magnetic fields. I discuss the time developments of particle distribution, electro-magnetic field, and the effect of nonlinear term in Yang-Mills equations. In the case of zero initial fields, hole structure in phase space was constructed as is the case with classical electro-magnetic(EM) plasma. This results shows the possibility that phenomena similar to classical electromagnetic plasma can be observed with small effects of nonlinear terms. In order to verify the applicability of various concepts in classical plasma, it is necessary to increase the accuracy and the spatial dimension of simulations.

Contents

Chapter 1

Introduction

In this chapter, I introduce background knowledge of my research.

1.1 Heavy ion collisions

Ultra-relativistic heavy ion collisions are extreme high energy physics on the earth. Experiments create quark gluon matter with high energy and density, called quark gluon plasma(QGP). It is considered that QGP was existed in the very beginning of the universe. Therefore, research of QGP dynamics has significant role for going way back to the early time physics. There are

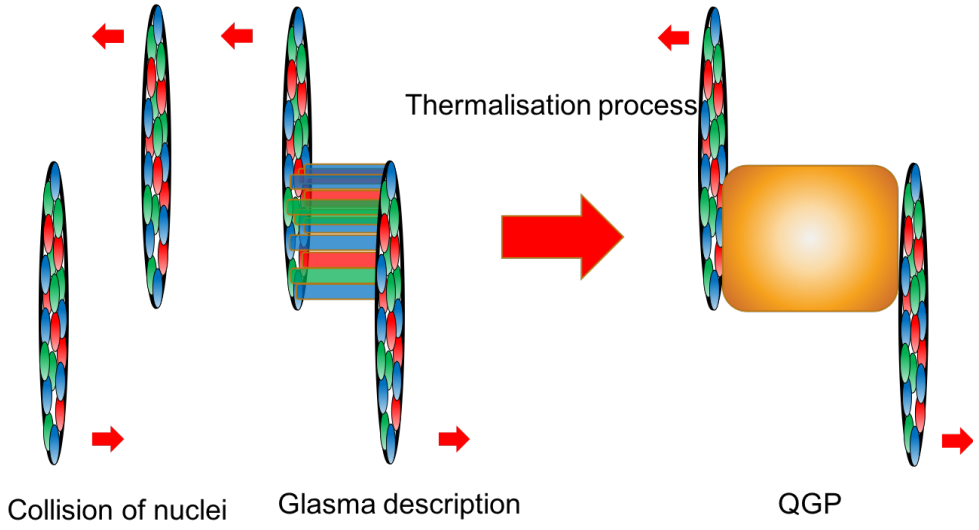

Figure 1.1: Time evolution of heavy ion collision.

several steps in heavy ion collisions as following: (1)First, accelerated nuclei at almost speed of light collide. They are pancake-like shape due to Lorentz

contraction.
(2)The energy density in the centre of collision get extremely high.
(3)Through thermalisation process, quarks and gluons go through phase transition to be in deconfined state.
(4)Haronisation occurs as the energy density decreases due to its expansion. Finally chemical freezeout takes place, then, kinds and number of hadron is determined.

1.2 Quark gluon plasma

QGP is deconfined state of quarks and gluons at extremely high temperature and energy density. Quarks and gluons are in confined state in hadronic sector, called hadron, however, phase transition to QGP takes place in extreme condition.
QGP is considered to be in local equilibrium state from experimental results. Lattice simulation[1] shows saturation of entropy density of quark gluon matter. Hydrodynamical simulation provide a good explanation for a

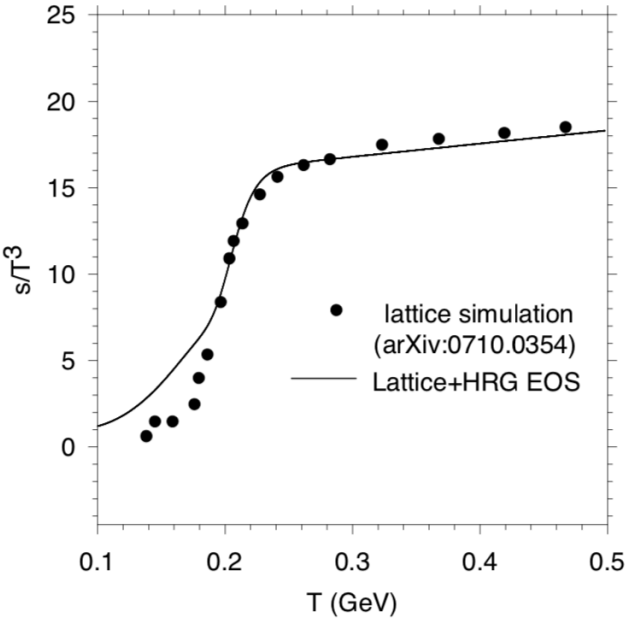

Figure 1.2: Entropy density saturate as time advances. It is one of the evidence of thermalisation of colliding nuclei[1]

lot of experimental data, such as radial and elliptic flow.

1.3 Colour glass condensate

QCD theory shows the possibility of asymptotic freedom in which the coupling constant decreases at the limit of high energy. In such weak coupling multi-body system, it is considered that a state called colour glass condensate exists. For such state, L. McLerran and R. Venugopalan gave a explanation, MV model[5]. This description tell that a lot of gluons are created in heavy ion collision due to its high energy density.
Fig1.3 show the parton distribution in proton while deep inelastic scatter-

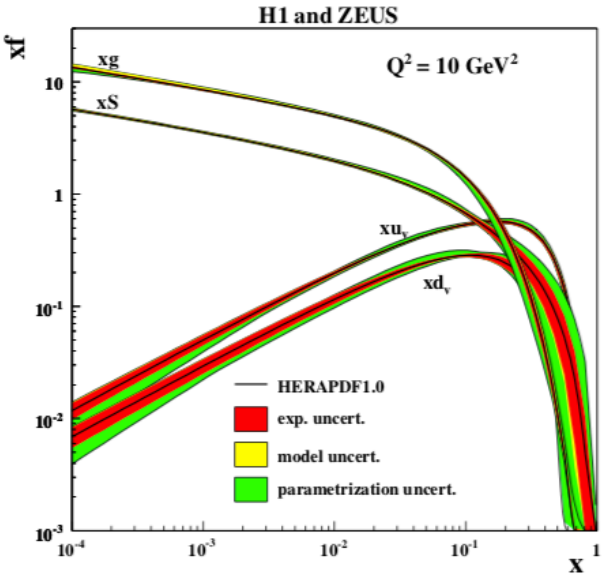

Figure 1.3: Parton distribution in proton, measured in deep inelastic scattering at HERA.[2]

ing at HERA. In fact, lattice calculation for parton distributions at high energy shows that gluons are outnumbering all the other particles. Therefore, valence quarks are negligible compared with gluons, and sea quarks are suppressed by one power of the coupling constant since they are produced from gluons $g \to q\bar{q}$.

1.4 Thermalisation process

One of the big question of heavy ion collision and creation of QGP is its thermalisation process of quark gluon matter. From Hydrodynamics, ther-

malisation time scale is about 0.6fm/c. However, calculation based on perturbative scattering show its time scale a few times larger than experimental data. One possible reason why scattering process estimate larger results is that this calculation ignores collective behavior of plasma, for example, plasma instabilities.

1.5 objective

The purpose of this thesis is to analyse the fundamental physics of non-Abelian plasma dynamics. The dynamics is important for investigating the mechanism of heavy ion collisions and the very beginning of the universe. Yang-Mills plasma dynamics for counter flow initial conditions are shown in this thesis.

Chapter 2

Basic concepts

2.1 Yang-Mills equations

I consider the system with only gluons because gluons occupy the centre part of collision and approximate the fields as classical one in the following. Because of low coupling constant, I divide into gluons with larger momentum and smaller momentum. In other words, I approximate gluons with large and small momentum to classical plasma particles and classical gauge fields, respectively. Metric of the system is (1,-1,-1,-1). Classical Yang-Mills equations in CGS unit is

$$\frac{1}{\sqrt{4\pi}}\partial_\nu F_a^{\mu\nu} - \frac{g}{\sqrt{4\pi}} f_{abc} A_\nu^b F_c^{\mu\nu} = -\sqrt{4\pi} g j_a^\mu \tag{2.1}$$

$$F_{\mu\nu}^a = \partial_\nu A_\nu^a - \partial_\nu^a - g f_{abc} A_\mu^b A_\nu^c, \tag{2.2}$$

where $F_a^{\mu\nu}$ is electro-magnetic tensor of gluon fields and A_ν^a is vector potential of gluon fields, j_a^μ is colour electric current. In addition, a is inertial degrees of freedom of gluons with 8 kinds for SU(3) theory. Here, letting $f(x, p, Q)$ be the distribution function in phase space for one particle, j_a^μ, $F_a^{\mu\nu}$ and A_ν^a are

$$j_a^\mu(x) = \int dpdQp^\mu Q_a f(x, p, Q) \tag{2.3}$$

$$\tag{2.4}$$

$$F_a^{\mu\nu} = \begin{pmatrix} 0 & E_x^a & E_y^a & E_z^a \\ -E_x^a & 0 & -B_z^a & B_y^a \\ E_y^a & B_z^a & 0 & -B_x^a \\ E_z^a & -B_y^a & B_x^a & 0 \end{pmatrix}$$

$$A^\nu = (\phi, \boldsymbol{A}). \tag{2.5}$$

I use these equations for colour particle simulations of gluon system. First, I discretise continuous distribution function into particles. Then f is

$$f(\boldsymbol{x}, \boldsymbol{p}, Q) = \frac{(2\pi)^3}{N_{test}} \sum_i \delta(\boldsymbol{x} - \boldsymbol{x}_i(t))\delta(\boldsymbol{p} - \boldsymbol{p}_i(t))\delta(Q - Q_i(t)), \tag{2.6}$$

where $\boldsymbol{x_i}(t), \boldsymbol{p_i}(t), Q_i(t)$ are position, momentum and colour charge of the ith particle. Therefore, colour electric current is

$$\boldsymbol{j}_a = g \sum_i Q_i^a \boldsymbol{v}_i \delta(\boldsymbol{x} - \boldsymbol{x}_i). \tag{2.7}$$

v_i is velocity of ith particle , and the absolute value is the same as light.
I use temporal gauge for gauge condition

$$A_0^a = 0. \tag{2.8}$$

From classical Yang-Mills equation and gauge condition,

$$\frac{\partial \boldsymbol{A^a}}{\partial t} = -\boldsymbol{E}^a \tag{2.9}$$

, and magnetic fields are

$$B_x^a = -\partial_z A_y^a + \partial_y A_z^a - g f_{abc} A_z^b A_y^c \tag{2.10}$$
$$B_y^a = -\partial_x A_z^a + \partial_z A_x^a - g f_{abc} A_x^b A_z^c \tag{2.11}$$
$$B_z^a = -\partial_y A_x^a + \partial_x A_y^a - g f_{abc} A_y^b A_x^c \tag{2.12}$$

Then, using $f_{abc} A_z^b A_y^c = -\frac{1}{2} f_{abc} [\boldsymbol{A}^b \times \boldsymbol{A}^c]_x$ from perfect antisymmetry of structure constant f_{abc}, colour magnetic field is

$$\boldsymbol{B^a} = \nabla \times \boldsymbol{A}^a + \frac{1}{2} g f_{abc} \boldsymbol{A}^b \times \boldsymbol{A}^c. \tag{2.13}$$

Substituting $\mu = 0$ into (2.2),

$$\partial_\nu F_a^{0\nu} - g f_{abc} A_\nu^b F_c^{0\nu} = -4\pi g j_a^0, \tag{2.14}$$

therefore, using $F_a^{00} = 0$,

$$\partial_1 F_a^{01} + \partial_2 F_a^{02} + \partial_3 F_a^{03} - g f_{abc} (A_1^b F_c^{01} + A_2^b F_c^{02} + A_3^b F_c^{03}) = -4\pi \rho_a. \tag{2.15}$$

This is Gauss's law for Yang-Mills equation.

$$\nabla \cdot \boldsymbol{E}^a + g f_{abc} \boldsymbol{A}^b \cdot \boldsymbol{E}^c = 4\pi \rho_a \tag{2.16}$$

Then, for the case of $\mu = 1$ (2.2) is

$$\partial_\nu F_a^{1\nu} - g f_{abc} A_\nu^b F_c^{1\nu} = -4\pi j_x^a \tag{2.17}$$

Substituting gauge condition and the values of fields, the x component is

$$\frac{\partial E_x^a}{\partial t} = \partial_y B_z^a - \partial_z B_y^a + g f_{abc}(A_y^b B_z^c - A_z^b B_y^c) - 4\pi j_x^a. \tag{2.18}$$

Adopting the same operation to $\mu = 2, 3$, we obtain

$$\partial_t \boldsymbol{E}^a = \nabla \times \boldsymbol{B}^a + g f_{abc} \boldsymbol{A}^b \times \boldsymbol{B}^c - 4\pi \boldsymbol{j}. \tag{2.19}$$

This is Ampere-Maxwell law of Yang-Mills equation. Then, differentiating eq.(2.13), we obtain

$$\partial_t \boldsymbol{B}^a = \nabla \times \partial_t \boldsymbol{A}^a + \frac{1}{2} g f_{abc}(\partial_t \boldsymbol{A}^b \times \boldsymbol{B}^c + \boldsymbol{A}^b \times \partial_t \boldsymbol{A}^c). \tag{2.20}$$

then,

$$\partial_t \boldsymbol{B}^a = -\nabla \times \boldsymbol{E}^a - g f_{abc} \boldsymbol{E}^b \times \boldsymbol{A}^c \tag{2.21}$$

This is Faraday's law of Yang-Mills equation. Finally, from the divergence of eq. (2.13), we obtain Gauss's law of magnetic field.

$$\nabla \cdot \boldsymbol{B}^a = -g f_{abc} \boldsymbol{A}^b \cdot \nabla \times \boldsymbol{A}^c \tag{2.22}$$

These equations and Maxwell equation are the same when the nonlinear term is zero. Therefore the nonlinear term is important for the dynamics of heavy ion collision.

2.2 Wong's equations

For large momentum gluons, I deal with them as plasma particle. In this section, I introduce the equations of motion for plasma particles.
Considering zero mass particles flying at the speed of light, the equation of motion, called Wong's equations are as follows.

$$\frac{d\boldsymbol{x}_i}{dt} = \boldsymbol{v}_i \tag{2.23}$$

$$\frac{d\boldsymbol{p}_i}{dt} = g Q_i^a (\boldsymbol{E}^a + \boldsymbol{v}_i \times \boldsymbol{B}^a) \tag{2.24}$$

$$\frac{dQ_i^a}{dt} = g f_{abc} \boldsymbol{v}_i \cdot \boldsymbol{A}^a Q_i^c \tag{2.25}$$

$$\boldsymbol{v} = \frac{\boldsymbol{p}}{\epsilon} \tag{2.26}$$

Here, ϵ is energy of particles.
One difference between classical Maxwell particles and colour particles is the time evolution of colour charge Q^a. For SU(N) gauge fields, Q^a satisfies the equation below.

$$Q^a Q_a = N. \tag{2.27}$$

The sum of colour charges is conservative for time evolution.

Chapter 3

Simulation methods

3.1 Particle-in-Cell method

To solve the motion of plasma particles, we need information of electromagnetic field at positions of particles. Particle positions are continuous, however, field is defined only on grids. In addition, we need to know electric current to solve equations showed in previous chapter.
Here, field F_p at particle position x_p is

$$F_p(x_p) = \sum_i F(x_i)S(x_i - x_p) = \sum_i F_i S_i(x_p), \tag{3.1}$$

using $F(x_i)$ defined on the grid. S is shape factor of particles. I use nearest grid point method in my research defined as below.

$$S = \begin{cases} 1 & if \frac{|x_p - x_i|}{\Delta x} \leq \frac{1}{2} \\ 0 & else \end{cases} \tag{3.2}$$

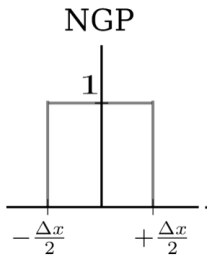

Figure 3.1: Nearest grid point method.

3.2 Discretisation of basic equations

In this section, I discretise basic equations in terms of Particle-in-Cell method. Basic equations are classical Yang-Mills equation for colour electro-magnetic fields and Wong's equations for motion of plasma particles.

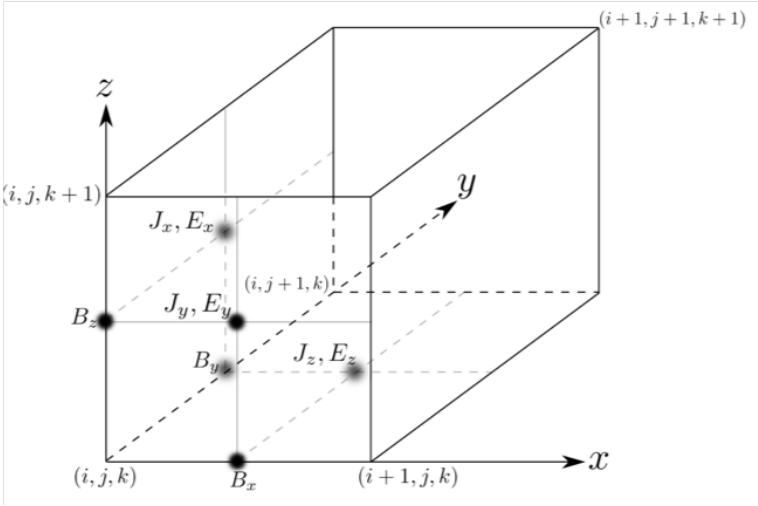

Figure 3.2: electro-magnetic fields on the grid.[4]

$$\frac{\partial \boldsymbol{A^a}}{\partial t} = -\boldsymbol{E}^a \tag{3.3}$$

$$\boldsymbol{B^a} = \nabla \times \boldsymbol{A}^a + \frac{1}{2}\epsilon_{abc}\boldsymbol{A}^b \times \boldsymbol{A}^c \tag{3.4}$$

$$\nabla \cdot \boldsymbol{E}^a + \epsilon_{abc}\boldsymbol{A}^b \cdot \boldsymbol{E}^c = \rho_a \tag{3.5}$$

$$\partial_t \boldsymbol{E}^a = \nabla \times \boldsymbol{B}^a + \epsilon_{abc}\boldsymbol{A}^b \times \boldsymbol{B}^c - \boldsymbol{j}. \tag{3.6}$$

$$\frac{d\boldsymbol{x}}{dt} = \boldsymbol{v} \tag{3.7}$$

$$\frac{d\boldsymbol{p}}{dt} = gQ^a(\boldsymbol{E}^a + \boldsymbol{v} \times \boldsymbol{B}^a) \tag{3.8}$$

$$\frac{dQ^a}{dt} = gf_{abc}\boldsymbol{v} \cdot \boldsymbol{A}^b Q^c \tag{3.9}$$

$$\boldsymbol{v} = \frac{\boldsymbol{p}}{\epsilon} = \frac{\boldsymbol{p}}{|\boldsymbol{p}|} \tag{3.10}$$

$$\frac{d\epsilon}{dt} = Q_a \boldsymbol{v} \cdot \boldsymbol{E}^a \tag{3.11}$$

Calculation step is as follows:
(1)update of electric fields
(2)update of vector potential
(3)update of magnetic fields

We can adopt central difference calculus:
-Assigning $\boldsymbol{E}, \boldsymbol{A}, \boldsymbol{j}$ to integer grids, $\boldsymbol{B}$ to half integer grids with respect to the spatial direction.
-Assigning $\boldsymbol{E}$ to integer grids, $\boldsymbol{Bj A}$ to half integer grids with respect to the time direction.
(i is spatial grid, n is time step)

$$\frac{E_{x,i}^{a,n} - E_{x,i}^{a,n-1}}{\Delta t} = \epsilon_{abc}(A_{y,i}^{b,n+\frac{1}{2}} B_{z,i}^{c,n+\frac{1}{2}} - A_{z,i}^{b,n+\frac{1}{2}} B_{y,i}^{c,n+\frac{1}{2}}) - j_{x,i}^{a,n+\frac{1}{2}} \quad (3.12)$$

$$\frac{E_{y,i}^{a,n} - E_{y,i}^{a,n-1}}{\Delta t} = -\frac{B_{z,i+\frac{1}{2}}^{a,n+\frac{1}{2}} - B_{z,i-]frac12}^{a,n+\frac{1}{2}}}{\Delta x} + \epsilon_{abc}(A_{z,i}^{b,n+\frac{1}{2}} B_{x,i}^{c,n+\frac{1}{2}} - A_{x,i}^{b,n+\frac{1}{2}} B_{z,i}^{c,n+\frac{1}{2}}) - j_{y,i}^{a,n+\frac{1}{2}} \quad (3.13)$$

$$\frac{E_{z,i}^{a,n} - E_{z,i}^{a,n-1}}{\Delta t} = -\frac{B_{y,i+\frac{1}{2}}^{a,n+\frac{1}{2}} - B_{y,i-]frac12}^{a,n+\frac{1}{2}}}{\Delta x} + \epsilon_{abc}(A_{x,i}^{b,n+\frac{1}{2}} B_{y,i}^{c,n+\frac{1}{2}} - A_{y,i}^{b,n+\frac{1}{2}} B_{x,i}^{c,n+\frac{1}{2}}) - j_{z,i}^{a,n+\frac{1}{2}}. \quad (3.14)$$

$$\frac{A_{x,i}^{a,n+\frac{1}{2}} - A_{x,i}^{a,n-\frac{1}{2}}}{\Delta t} = -E_{x,i}^{a,n} \quad (3.15)$$

$$\frac{A_{y,i}^{a,n+\frac{1}{2}} - A_{y,i}^{a,n-\frac{1}{2}}}{\Delta t} = -E_{y,i}^{a,n} \quad (3.16)$$

$$\frac{A_{z,i}^{a,n+\frac{1}{2}} - A_{z,i}^{a,n-\frac{1}{2}}}{\Delta t} = -E_{z,i}^{a,n}. \quad (3.17)$$

$$B_{x,i+\frac{1}{2}}^{a,n+\frac{1}{2}} = \frac{1}{2}\epsilon_{abc}(A_{y,i+\frac{1}{2}}^{b,n+\frac{1}{2}} A_{z,i+\frac{1}{2}}^{c,n+\frac{1}{2}} - A_{z,i+\frac{1}{2}}^{b,n+\frac{1}{2}} A_{y,i+\frac{1}{2}}^{c,n+\frac{1}{2}}) \quad (3.18)$$

$$B_{y,i+\frac{1}{2}}^{a,n+\frac{1}{2}} = -\frac{A_{z,i+\frac{1}{2}}^{a,n+\frac{1}{2}} - A_{z,i-\frac{1}{2}}^{a,n+\frac{1}{2}}}{\Delta x} - \frac{1}{2}\epsilon_{abc}(A_{z,i+\frac{1}{2}}^{b,n+\frac{1}{2}} A_{x,i+\frac{1}{2}}^{c,n+\frac{1}{2}} - A_{x,i+\frac{1}{2}}^{b,n+\frac{1}{2}} A_{z,i+\frac{1}{2}}^{c,n+\frac{1}{2}}) \quad (3.19)$$

$$B_{z,i+\frac{1}{2}}^{a,n+\frac{1}{2}} = -\frac{A_{y,i+\frac{1}{2}}^{a,n+\frac{1}{2}} - A_{y,i-\frac{1}{2}}^{a,n+\frac{1}{2}}}{\Delta x} - \frac{1}{2}\epsilon_{abc}(A_{x,i+\frac{1}{2}}^{b,n+\frac{1}{2}} A_{y,i+\frac{1}{2}}^{c,n+\frac{1}{2}} - A_{y,i+\frac{1}{2}}^{b,n+\frac{1}{2}} A_{y,i+\frac{1}{2}}^{c,n+\frac{1}{2}}). \quad (3.20)$$

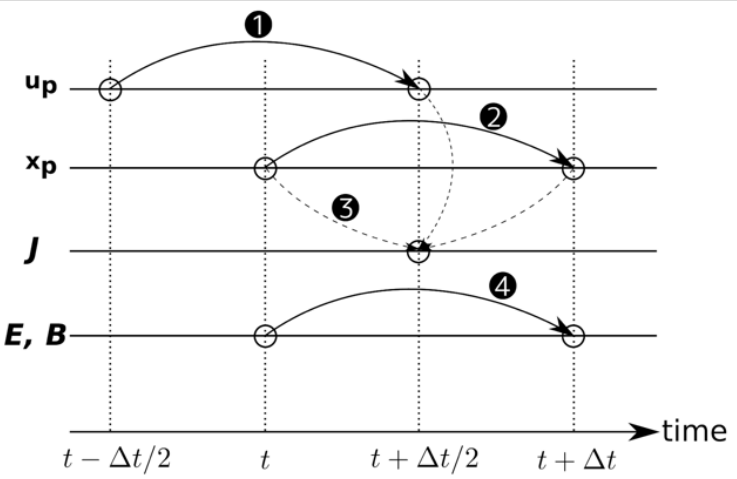

Figure 3.3: Updates of physical values.[4]

Then, I discretise the equation of motion of particle. We can adopt central calculus:
-Assigning $Q_a, \boldsymbol{x}, \epsilon$ to integer grids, $\boldsymbol{p}, \boldsymbol{v}$ to half integer grids with respect to the time direction.

$$\frac{\boldsymbol{p}^{n+\frac{1}{2}} - \boldsymbol{p}^{n-\frac{1}{2}}}{\Delta t} = Q_a^n(\boldsymbol{E}_a^n + \boldsymbol{v}^n \times \boldsymbol{B}_a^n) + O(\Delta t^2) \tag{3.21}$$

We can obtain the values at integer time steps using backward difference.

$$\boldsymbol{p}^n = \frac{\boldsymbol{p}^{n+\frac{1}{2}} - \boldsymbol{p}^{n-\frac{1}{2}}}{2} + O(\Delta t^2) \tag{3.22}$$

$$\boldsymbol{v}^n = \frac{\boldsymbol{p}^n}{|\boldsymbol{p}^n|}. \tag{3.23}$$

By backward difference, particle energy is

$$\frac{\epsilon^n - \epsilon^{n-1}}{\frac{\Delta}{2}} = Q_a^n \boldsymbol{v} \cdot \boldsymbol{E}_a^n + O(\Delta t). \tag{3.24}$$

Substituting $\boldsymbol{v}^n = \boldsymbol{v}^{n-\frac{1}{2}} + O(\Delta t)$, we obtain

$$\epsilon^n = \epsilon^{n-\frac{1}{2}} + \frac{1}{2} Q_a^n \Delta t \boldsymbol{v}^{n-\frac{1}{2}} \cdot \boldsymbol{E}_a^n + O(\Delta t^2). \tag{3.25}$$

Particle position is also obtained.

$$\boldsymbol{x}^{n+1} = \boldsymbol{x}^n + \boldsymbol{v}^{n+\frac{1}{2}} \Delta t + O(\Delta t^2) \tag{3.26}$$

The difference between classical electro-magnetic plasma and Yang-Mills plasma is time evolution of colour charge.

$$\frac{Q_a^{n+1} - Q_a^n}{\Delta t} = \epsilon_{abc} \boldsymbol{v}^{n+\frac{1}{2}} \cdot \boldsymbol{A}_b^{n+\frac{1}{2}} Q_c^{n+\frac{1}{2}} \tag{3.27}$$

3.3 Colour-electric current on a grid

We need to define electric current and charge density on grids because the fields are defined only on grids. I define electric current in this section. Electric current for ith particle with colour a is defined as

$$\boldsymbol{j}_a = g \sum_i Q_i^q \boldsymbol{v}_i \delta(\boldsymbol{x} - \boldsymbol{x}_i). \tag{3.28}$$

Defining shape factor S

$$S_{i,k} = \int_\Delta V_k S_0(\boldsymbol{x} - \boldsymbol{x}_i) dx, \tag{3.29}$$

I define electric current on grid k as the mean value of the cell. Then, we obtain

$$\boldsymbol{j}_k^a = \frac{g}{\Delta V_k} \sum_i Q_i^a \boldsymbol{v}_i S_{i,k}. \tag{3.30}$$

Chapter 4

Results

4.1 Results without nonlinear effects

In this section, I show some results for classical Maxwell plasma to justify the program. For this purpose I use pcans[2] code.
I employ electron-electron two steam instability. Two components of electron fluid have relative velocity, and there are finite mass ion in the background in initial condition. To, analyse the instability, wave number in the boundary of two components is important. When instability grows, large wave number components increase in Fourier expansion. I obtained the results of growth curve from simulation and theory. I adopt Fourier expansion to mode four and five with respect to space components.

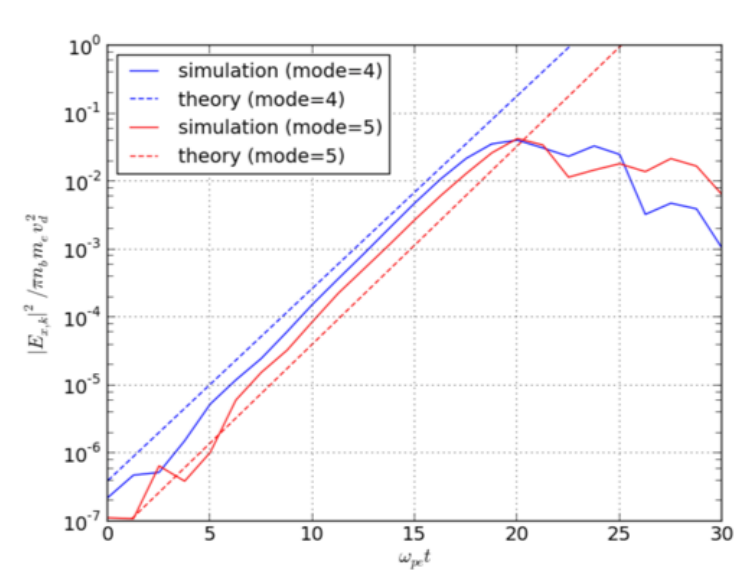

Figure 4.1: Growth curve for mode 4,5. [4]

This results shows that calculation agrees the theoretical results. It justifies results using my program.

4.2 Results for Yang-Mills plasma

In this section, I provide results for classical Yang-Mills plasma. Here, I employ simple initial condition 1,2. initial condition 1 has zero initial fields, and 2 has finite electric field for x direction.

Table 4.1: initial condition 1

direction	x	y	z
electric field E	0	0	0
magnetic field B	0	0	0
vector potential A	0	0	0

Table 4.2: initial condition 2

direction	x	y	z
electric field E	0.5	0	0
magnetic field B	0	0	0
vector potential A	0	0	0

Initial position distribution of particles are given uniformly and velocity distribution is given by Maxwell distribution by random numbers in both conditions.

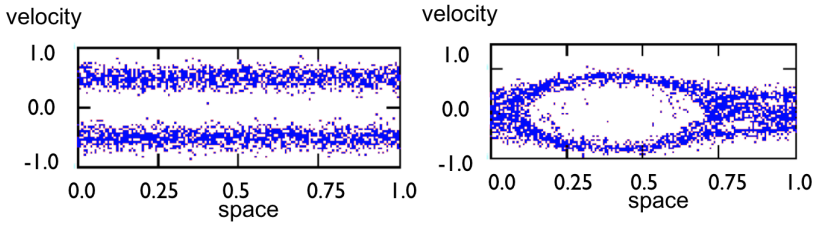

Figure 4.2: left: initial distribution of particles in phase space. right: distribution at t=200.

This result shows that there is a hole structure in phase space as is the case of classical Maxwell plasma. It indicates the existence of hole in heavy ion collision.

Hole structures of classical electro-magnetic plasma are shown in recent research[8]. To, confirm whether the structure exist, multi-dimentional simulations are necessary. Plasma hole is one the significant topic for this research.

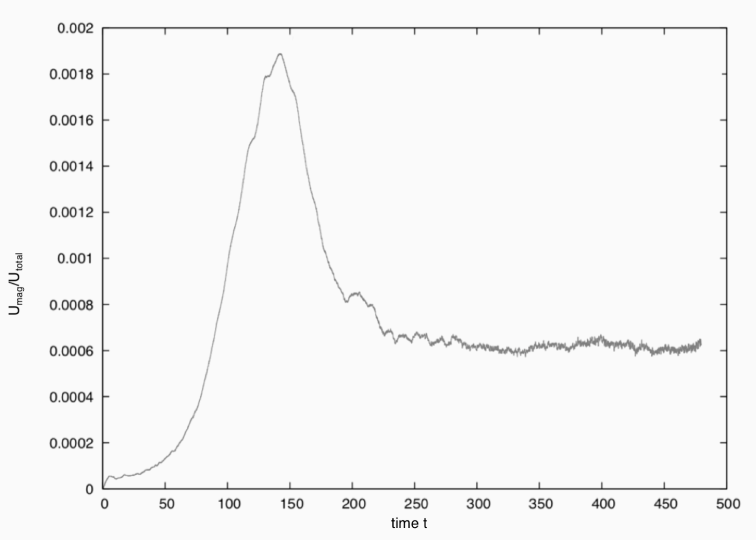

Figure 4.3: Time evolution of energy of electro-magnetic fields vs. total energy.

In Figure4.3, the time evolution of energy ratio of electro-magnetic fields and total energy is shown. At first, the energy rise quickly, and then, decrease to relaxation. Further work need to analyse the linear growth of its evolution to make sure which instability takes place.

Figure4.4 shows the time evolution of energy ration of electro-magnetic fields and total energy. Blue is the result with initial condition 2. Green and black show the results with initial condition 1 and without nonlinear terms of Yang-Mills equations and with initial condition 1 respectively. In these results, no significant differences cannot be confirmed.

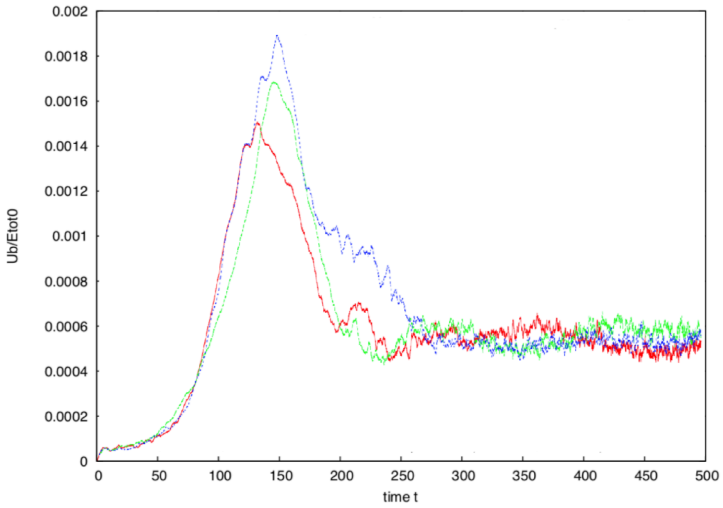

Figure 4.4: Time evolution of energy of electro-magnetic fields vs. total energy. Blue: with finite initial electromagnetic fields. Green: with zero initial fields. Black: without nonlinear terms of Yang-Mills equations and with zero initial fields.

Chapter 5

Conclusion

I study the fundamental physics of classical Yang-Mills plasma dynamics. This is the key to analyse the thermalisation process of heavy ion collisions. I employ initial condition which has counter flow of particles. The results shows the existence of hole structure which is obtained in simulations of classical Maxwell plasma with weak initial fields.
It is reported that plasma hole can be shown not only in simulation but also in realistic phenomena. In this thesis, the possibility that there are hole structure in thermalising plasma in heavy ion collisions. In addition, shock waves in collisionless plasma[9] are valuable topic to analyse. Thermalising gluon plasma can be regarded as collisionless plasma. Therefore, there is possibility that shock wave exist in such plasma and it can affect the thermalisation process of heavy ion collisions.
For future prospectives, it is necessary to increase the accuracy and spatial dimension of simulations for more various research including realistic initial conditions. To analyse specific phenomena such as collisionless shock and plasma hole, we need to expand spatial region and spatial dimension of simulations.

Acknowledgements

I would like to thank my supervisor Dr.Takahiro Miyoshi for discussion and advice of research. I acknowledge all staffs in Quark physics laboratory, Prof. Toru Sugitate, Prof. Kenta Shigaki and Dr.Kensuke Homma. All staffs and members of laboratory gave me a lot of important suggestions at the meeting.

Bibliography

[1] A. K. Chaudhuri, "Centrality dependence of elliptic flow and QGP viscosity", arXiv:0910.0979v3 [nucl-th] (2010).

[2] F. Gelis, "Color Glass Condensate and Glasma" , arXiv:1211.3327v2 [hep-ph].

[3] Wong, S. K., "Field and particle equations for the classical Yang-Mills field and particles with isotopic spin", https://doi.org/10.1007/BF02892134.

[4] http://www.astro.phys.s.chiba-u.ac.jp/pcans/.

[5] Dumitru, Adrian and Nara, Yasushi and Strickland, Michael, "Ultraviolet avalanche in anisotropic non-Abelian plasmas", 10.1103/PhysRevD.75.025016(2007).

[6] Adrian Dumitru,Yasushi Nara,Phys.Lett.B,621,(2005)89-95.

[7] Takashi Okazaki,"Plasma Heating by a Relativistic Electron Beam. II. Two-Stream and Return Current Driven Instabilities",Journal of the Physical Society of Japan, 49, 1532-1541 (1980).

[8] I. H. Hutchinson, "Electron holes in phase space: What they are and why they matter",Physics of Plasmas 24, 055601 (2017).

[9] G. K. Parks, E. Lee, S. Y. Fu, N. Lin, Y. Liu, Z. W. Yang,"Shocks in collisionless plasmas", Reviews of Modern Plasma Physics 10.1007/s41614-017-0003-4(2017).